Are Hydrogen-Bonded Charge Transfer Crystals Room Temperature Ferroelectrics?

Gabriele D'Avino* and Matthieu J. Verstraete

Université de Liège, Institut de Physique, and European Theoretical Spectroscopy Facility, Allée du 6 Août 17, Sart-Tilman, B-4000 Liège, Belgium

(Received 5 June 2014; published 3 December 2014)

We present a theoretical investigation of the anomalous ferroelectricity of mixed-stack charge transfer molecular crystals, based on the Peierls-Hubbard model, and first-principles calculations for its parametrization. This approach is first validated by reproducing the temperature-induced transition and the electronic polarization of TTF-CA, and then applied to a novel series of hydrogen-bonded crystals, for which room temperature ferroelectricity has recently been claimed. Our analysis shows that the hydrogen-bonded systems present a very low degree of charge transfer and hence support a very small polarization. A critical reexamination of experimental data supports our findings, shedding doubts on the ferroelectricity of these systems. More generally, our modeling allows the rationalization of general features of the ferroelectric transition in charge transfer crystals and suggests design principles for materials optimization.

DOI: 10.1103/PhysRevLett.113.237602 PACS numbers: 77.80.-e, 71.10.Fd, 71.20.Rv, 71.30.+h

Mixed-stack charge transfer (CT) crystals (e.g., TTF-CA, TTF-BA) are a spectacular example of multifunctionality in organic materials. Being one of the few examples of quantum ferroelectricity among organics [1–4], CT crystals offer novel opportunities to achieve magnetoelectric control of the polarization [5], and for the realization of ultrafast nonlinear optical oscillators [6]. Moreover, the occurrence of photoinduced phase transitions [7] triggered by multi-excitonic phenomena [8,9] make these systems interesting for optical switching, memory, and energy generation applications.

This intriguingly rich physics emerges from a quite simple structure, in which electron-donor (D) and -acceptor (A) molecules pack in an alternating one-dimensional (1D) pattern $D^{+\rho}A^{-\rho}D^{+\rho}A^{-\rho}$ characterized by a fractional charge transfer ρ [see Fig. 1(a)]. Both neutral (N, $\rho \lesssim 0.5$) and ionic (I, $\rho \gtrsim 0.5$) CT crystals are known, and a few of them can undergo the so-called N-I transition, from a N phase to a low-temperature (T) and high-pressure I phase [10–12]. In I systems a generalized Peierls instability may lead to a dimerization of the lattice and ferroelectric phases characterized by an exceptionally strong electronic polarization, pointing antiparallel to molecular displacement dipoles [3].

The archetypical organic CT ferroelectrics are the complexes of the tetratiafulvalene-halo- p-benzoquinone (TTF-QBr_xCl_{4-x}) family, presenting transition temperatures $T_c = 81$, 67, and 53 K for $x = 0$ (TTF-CA), $x = 1$, and $x = 4$ (TTF-BA), respectively [1]. Room-temperature ferroelectricity has recently been reported in a novel series of CT crystals characterized by the presence of a supramolecular network of hydrogen bonds [H-bonded charge transfer (HBCT), see Fig. 1] [13]. This seems to pave the way for their application in realistic all-organic devices. Remarkably, CT and H bonds, two phenomena which both possibly lead to ferroelectricity in molecular systems [1,14,15], coexist in HBCT.

In this Letter, by means of a novel theoretical approach based on a model Hamiltonian fed with first-principles inputs, we discuss on equal footing TTF-CA and HBCT, to determine the origin of the unprecedented properties of the latter and provide general insights on the anomalous ferroelectricity of mixed-stack CT crystals.

Electronic and structural instabilities of CT crystals are described by the 1D modified Hubbard Hamiltonian with electron-phonon coupling [16,17], which, in conjunction with the modern theory of polarization in dielectrics [18],

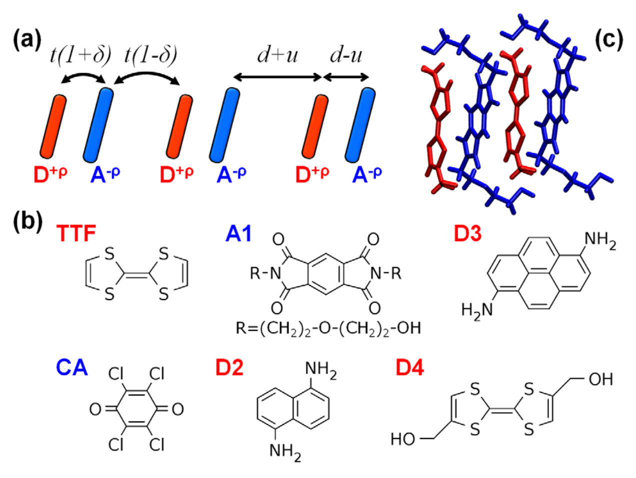

FIG. 1 (color online). (a) Sketch of a dimerized mixed stack with alternating CT integrals and molecular displacements (exaggerated for clarity). (b) Chemical structures of D (red) and A (blue) molecules considered in this work. HBCT are complexes formed by the same acceptor, $A1$, and the three different donors, $D1$, $D2$, and $D3$. (c) Perspective view of molecular packing in the $A1$-$D4$ crystal.

provides a coherent framework that explains the divergence of the dielectric constant [19,20], vibrational spectra [12,21], and diffuse x-ray data [22]. The physics of CT crystals is captured in its essence by the infinite-correlation limit [23] of the modified Peierls-Hubbard (MPH) Hamiltonian:

$$H = \Gamma_{\rm eff}\sum_i(-1)^i\hat{n}_i - t\sum_{i,\sigma}[1+(-1)^i\delta]\hat{b}_{i,\sigma} + \frac{Nt^2}{2\epsilon_\delta}\delta^2, \quad (1)$$

where $\Gamma_{\rm eff}$ is the effective ionization gap of a DA pair, t is the CT integral, δ is the dimensionless coordinate of the Peierls mode, with relaxation energy ϵ_δ, $\hat{b}_{i,\sigma} = (c^\dagger_{i,\sigma}c_{i+1,\sigma} + \mathrm{H.c.})$ is the bond-order operator, and N is the number of sites. Hamiltonian (1) describes a continuous transition from a neutral band-insulating to an ionic Mott-insulating state upon decreasing $\Gamma_{\rm eff}$. At the critical point, characterized by a divergent polarizability, the instability to lattice dimerization becomes unconditional, so that the I phase is always polar at $T = 0$.

A more realistic model for CT crystals can be obtained by including electrostatic interactions in the 3D solid and intramolecular Holstein vibrations, allowing us to describe discontinuous N-I transitions [16,17]. A mean-field treatment of electrostatic interactions leads to the self-consistent 1D Hamiltonian:

$$H_{\rm CT} = \left(\Gamma + \frac{V}{2} + q + \epsilon_c\rho\right)\sum_i(-1)^i\hat{n}_i - t\sum_{i,\sigma}[1+(-1)^i\delta]\hat{b}_{i,\sigma} + \frac{Nt^2}{2\epsilon_\delta}\delta^2 + \frac{Nt^2}{2\epsilon_q}q^2 \quad (2)$$

plus constant terms [17]. Here, 2Γ is the energy to ionize a DA pair at infinite distance and V is the nearest-neighbor electrostatic interaction, q is the coordinate of the Holstein mode, with relaxation energy ϵ_q, and $\epsilon_c = 2M - V$, where M is the Madelung energy measuring the total strength of electrostatic interactions.

Traditionally, the model parameters were derived from experiments [17,24] and empirical relationships between $\Gamma_{\rm eff}$ or V and T (or pressure) were established in order to induce the N-I transition [21,22]. In this work we instead propose a novel and general approach to the parametrization of Hamiltonian (2) based on density functional theory (DFT). This strategy is first validated by reproducing the T-induced N-I transition of TTF-CA, and then it is applied to the series of HBCT crystals.

The values of t, δ, and $\Gamma' = \Gamma + V/2$ are obtained by mapping DFT calculations on DA dimers to the corresponding effective model. We perform DFT calculations on nearest-neighbor DA dimers extracted from the crystal structures (at different T for TTF-CA) [13,25,26] and compute energy and intermolecular CT in the singlet (ρ_1) and triplet (ρ_3) ground states. We adopt three recent hybrid functionals, CAM-B3LYP, ωB97X, and M06-HF as implemented in the GAUSSIAN09 suite [27]. ρ_1 and ρ_3 were evaluated with natural population analysis atomic charges [28].

On the other hand, in the strong-correlation limit [23] the modified Hubbard Hamiltonian for a DA dimer factorizes into a two-state model for the singlet subspace, plus three fully-CT ($\rho_3 = 1$) triplet states that are unaffected by the CT interaction [see Fig. 2(a)]. This simple analytical model is fully characterized by the two parameters t and Γ', whose values can be obtained from closed expressions in terms of the singlet-triplet gap $\Delta_{\rm ST}$ and the singlet ground-state CT ρ_1, calculated with DFT. By considering the symmetry inequivalent dimers in polar stacks, one can access both t and δ [29].

The values of t, δ, and Γ' for TTF-CA and HBCT are shown in Figs. 2(b) and 2(c). For TTF-CA we obtain a nearly T-independent t and comparable results for different functionals, with CAM-B3LYP achieving a quantitative agreement with previous empirical estimates, $t \sim 0.21$ eV [24]. Γ' shows an increasing trend with temperature, ascribable to the weakening of the nearest-neighbor interaction V with the lattice expansion.

A very different scenario emerges for HBCT crystals, which are characterized by t values comparable to TTF-CA, smaller dimerizations ($\delta < 0.1t$), and, most importantly, values of Γ' more than 0.5 eV larger than in TTF-CA. The last result is clearly due to the weak DA character of HBCT complexes, as also confirmed by experimental [10,13] and calculated redox potentials [29].

The other crucial parameters entering Hamiltonian (2) are those quantifying electrostatic interactions in the solid.

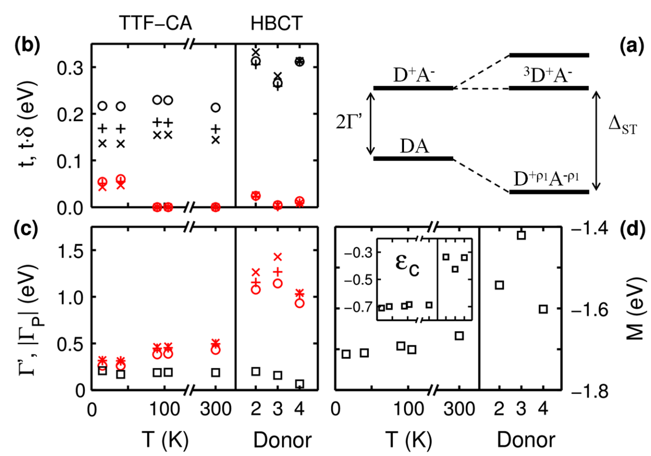

FIG. 2 (color online). Model parameters calculated for TTF-CA and HBCT. (a) Sketch of the energy levels for a DA dimer. Values of (b) t (black symbols), $t\delta$ [red (gray) symbols] and (c) $\Gamma' = \Gamma + V/2$ [red (gray) symbols] obtained from CAM-B3LYP (circles), ωB97X (pluses), and M06-HF (crosses) functionals and $6\text{–}31+\mathrm{G}^*$ basis set. Squares correspond to the environment polarization contribution to the DA ionization energy, $\Gamma_P < 0$. (d) Madelung energy, M, and ϵ_c (inset).

M and ε_c are here evaluated with a point-charge model, in which dielectric screening is accounted for with a microscopic model for molecular polarization, based on DFT inputs [29–31].

The computed values of M, shown in Fig. 2(d), are large and negative as foreseeable for ionic lattices. The Madelung energy decreases in magnitude with T in TTF-CA, confirming the expected gain in electrostatic energy upon lattice contraction. Smaller $|M|$ values are found for HBCT: the difference with respect to TTF-CA is ascribable to the looser molecular packing in the presence of side chains.

The polarization of the environment is also responsible for a renormalization of the crystal ionization gap with respect to its gas-phase value; i.e., $\Gamma \rightarrow \Gamma + \Gamma_P$ [29]. Γ_P [squares in Fig. 2(c)] has been evaluated to be about -0.2 eV [29].

With the set of parameters at hand, we can now perform MPH calculations specific for TTF-CA and HBCT. As in previous works [17,21], Hamiltonian (2) is diagonalized exactly for chains with $N = 16$ sites and periodic boundary conditions. 3D electrostatic interactions are treated at the mean-field level. The Peierls phonon coordinate δ is set to the values determined from experimental structures [see Fig. 2(b)], while the Holstein coordinate is relaxed [32]. In the following, we will show results obtained with the CAM-B3LYP estimates of t, δ, and Γ. The other functionals provide similar results [29].

Calculated and experimental ionicity across the N-I transition of TTF-CA are shown in Fig. 3(a). Our

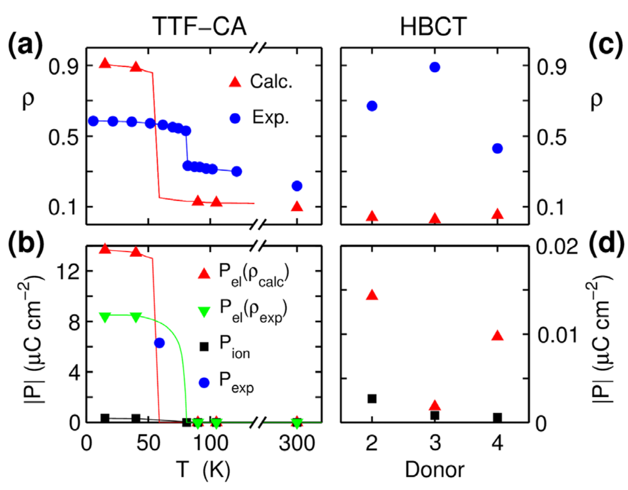

FIG. 3 (color online). Ground-state ionicity and polarization of TTF-CA and HBCT calculated with the MPH model and CAM-B3LYP parameters in Fig. 2 (data points). Higher T resolution for TTF-CA (lines) is obtained with diagonalizations for interpolated values of the parameters. The calculations describe (a) the T-induced N-I transition of TTF-CA and (b) the direction and magnitude of the polarization. Unlike in Ref. [13], all HBCT crystals are found to be largely N (c) and with negligible P (d) (see text).

calculations describe the first-order transition of TTF-CA without adjustable parameters, locating the critical point in the correct T range. Although the ionicity jump at the transition is overestimated, this result confirms the common picture of this transition: TTF-CA lies close to the N-I boundary, where a small increase in the Madelung energy drives the system from the N to the I phase.

The polarization along the stack (crystal axis a in TTF-CA) can be decomposed in an electronic contribution $P_{\rm el}$ and an ionic one $P_{\rm ion}$. According to the modern theory of polarization, $P_{\rm el}$ is computed as a Berry phase [18,20]:

$$P_{\rm el} = \frac{ed}{\pi\Omega} \operatorname{Im} \ln \langle \Psi | \exp\left(i \frac{2\pi \hat{M}}{N} \right) | \Psi \rangle, \qquad (3)$$

where Ψ is the many-body ground state, $\hat{M}$ is the dipole moment operator of the open-boundary chain, d is the intermolecular distance (at $\delta = 0$), Ω is the volume per DA pair, and e is the elementary charge. The ionic contribution, due to frozen charges $\pm\rho$ at molecular sites displaced by u [see Fig. 1(a)], is $P_{\rm ion} = e\rho u/\Omega$.

The electronic polarization computed for TTF-CA, shown in Fig. 3(b), is of the order of magnitude of experimental values ($6.3\ \mu\mathrm{C\,cm^{-2}}$ at 51 K [3]), and correctly points antiparallel to the almost negligible ionic contribution, as also reported by Giovannetti *et al.* [33]. $P_{\rm el}$ is evaluated at both the calculated and experimental ionicity, showing a very good agreement with experiments in the second case. This allow us to conclude that, apart from inaccuracies in the estimation of ρ, the MPH model provides a quantitative description of the electronic polarization of CT crystals. The better result obtained for $P_{\rm el}$ with respect to the previous *ab initio* attempts [33,34] suggests that an explicit, though approximate, treatment of the strong correlations seems to be more important than other details of the electronic structure.

MPH calculations for HBCT predict all of the three crystals to be largely neutral ($\rho < 0.1$) and characterized by very small polarizations [see Figs 3(c) and 3(d)]. This is in marked contrast with the results of Ref. [13], where HBCT crystals were attributed ρ values spanning a range of 0.4–0.9 and polarization comparable to or higher than TTF-CA. The discrepancy between experiment and theory is addressed in the following.

Experimental estimates of ρ in CT crystals rely on the approximately linear dependence of the frequency of asymmetric $\mathrm{C=O}$ stretchings on the molecular charge, as it is well established for CA complexes [35]. A similar procedure has been used for HBCT in Ref. [13], where a tiny *hardening* of the $\mathrm{C=O}$ mode of $A1$, $\Delta\tilde{\nu} = \tilde{\nu}^- - \tilde{\nu}^0 = 14\ \mathrm{cm^{-1}}$, has been ascribed to the complete molecular ionization. This is at odds with what is observed in CA, where, in agreement with chemical intuition, the relevant bond strongly *weakens* in ionized molecules ($\Delta\tilde{\nu} = -160\ \mathrm{cm^{-1}}$) [35]. Normal mode calculations on neutral and charged molecules yield $\Delta\tilde{\nu} = -198$ and -89 cm^{-1} in CA and $A1$, respectively [29]. This leads us to conclude that the ρ values of HBCT crystals are actually very similar and quite small.

Further confirmation of our ionicity estimates can be found by considering the whole experimental scenario. The relationship between ρ, the frequency of the CT optical transition ω_{CT}, and the difference between the redox potentials of D and A, ΔE_r, has been established in Torrance's V-shaped diagram, which has been empirically validated for many CT crystals [10]. While TTF-CA lies at the boundary between N and I phases, the experimental values reported for HBCT ($\omega_{\mathrm{CT}} \sim 1.4$–$1.8$ eV and $\Delta E_r \sim 1.1$–1.6 eV [13]) safely locate these systems in the N region.

The polar crystal structures of HBCT were obtained by refining low-T (84–100 K) x-ray diffraction data in noncentrosymmetric space groups. The only argument brought in support of the room-T polarity of these systems is the violation of the mutual exclusion rule in IR and Raman spectra [13]. However, for HBCT there is no evidence of the very intense vibronic bands characterizing the IR spectra of dimerized stacks [35]. The coincidence of Raman and weak IR bands in busy vibrational spectra (because of the presence of side chains) should be considered accidental rather than a proof of the polarity of HBCT.

Finally, the polarization hysteresis loops of the HBCT crystals at room temperature show neither saturation nor reproducibility. These features are reminiscent of artifacts due to leakage current [36,37], which are indeed mentioned to occur in HBCT, especially at high T [13]. Moreover, we note that the remnant polarization reported for $A1$-$D4$ is 1 order of magnitude higher than the upper limit prescribed by the modern theory of polarization for one-electron transfer. Both theory and experiments cast doubts on the ferroelectricity of HBCT, calling for an unambiguous proof of the structure polarity and cleaner dielectric measurements.

In order to offer a comprehensive picture of the ferroelectric transition in CT crystals, we now present the general properties of the charge and lattice instability of the MPH model. This provides useful guidelines for achieving robust ferroelectrics with high T_c. As is well known, the increase of ρ triggers the lattice instability, and the ground-state potential in Fig. 4(a) develops a double well. The minima at $\pm\delta_{\mathrm{eq}}$ correspond to polar phases of opposite polarization [16,17]. The depth of the wells [ΔE in Fig. 4(b)] determines the stability of the polar phase against thermal fluctuations. ΔE increases with the lattice softness and reaches a maximum at $\rho \sim 0.6$. In this regime, the lattice instability has a Peierls-like mechanism, with delocalized electrons forming a bond-order charge density wave. Conversely, the spin-Peierls instability of localized spins in the Mott-insulating I phase results in vanishing ΔE

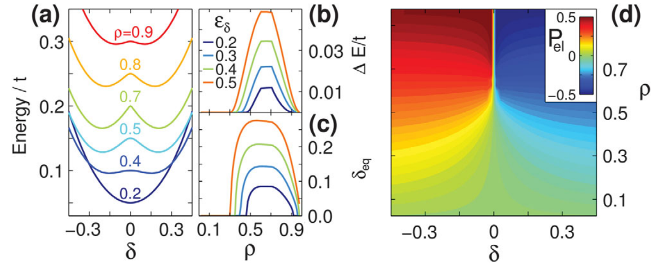

FIG. 4 (color). (a) Ground-state energy of Hamiltonian (1) as a function of δ for different values of ρ and $\epsilon_\delta = 0.4t$. Panels (b) and (c) show the depth of the double well and the equilibrium position as a function of ρ for different ϵ_δ. (d) Electronic polarization (dipole moment per molecule in ed units) of the MPH model as a function of ρ and δ.

in the $\rho = 1$ limit. This explains why TTF-BA, featuring $\rho = 0.95$ up to room T, dimerizes only below 53 K, while higher transition temperatures are observed for TTF-CA and TTF-QBrCl$_3$, which both undergo ferroelectric transitions to I phases with $\rho \sim 0.55$.

The magnitude of the electronic polarization is determined by the ionicity and the dimerization amplitude, as shown in Fig. 4(d). P_{el} is an odd function of δ and vanishes by symmetry in the regular stack. P_{el} remains small at low ionicities, while for $\rho > 0.6$ it becomes large and discontinuous at $\delta = 0$. Sizable CT ($\rho \gtrsim 0.3$) is therefore an essential requisite to obtain a strong electronic polarization, which is instead less sensitive to the dimerization amplitude. Large and nonlinear variations of P_{el} with δ are signatures of the strong entanglement of correlated, yet delocalized, electrons with vibrations, suggesting that the concept of Born effective charges should be used with caution in these systems.

Hydrogen bonds can alter this picture by affecting the crystal packing (e.g., by favoring polar phases) or by being responsible for an additional contribution to the polarization, as reported for several single- and multicomponent H-bonded ferroelectrics [1,14,15]. Our calculations account only for the structural effect on CT through the evaluation of the model parameters at experimental geometries. The polarization of H-bonded ferroelectrics originates from the rearrangement of the π-conjugated electron system (tautomerism) associated with a reversible and collective proton transfer [1,14,15,38]. Since the weak H bonds of HBCT, involving atoms on saturated alkyl chains, cannot imply similar phenomena, we exclude the possibility that they could be responsible for the discrepancy between our estimate for the polarization and the data in Ref. [13].

In conclusion, we present a novel and general approach to the modeling of mixed-stack CT crystals, which is able to capture the anomalous electronic ferroelectricity of TTF-CA. We show that the novel HBCT complexes are all characterized by very low ionicities, as confirmed by a close reading of the original experimental data. The latter do not unambiguously demonstrate the presence of ferroelectricity. More generally, the theoretical framework we propose for CT crystals, by allowing one to target chemical specificity while fully accounting for the strong electronic correlations, is a powerful tool for the comprehension of the complex physics governing these promising multifunctional materials.

G. D. gratefully acknowledges enlightening discussions with Anna Painelli, Alberto Girlando, and Matteo Masino. We thank Eric Bousquet for carefully reading the manuscript. This research was supported by the University of Liege and the EU in the context of the FP7-PEOPLE-COFUND-BEIPD project. The authors acknowledge an Action de Recherches Concertée (A. R. C.) grant (TheMoTherm 10/15-03) and a Fonds de la Recherche Fondamentale Collective (FRFC) grant (Attosecond control of electron dynamics 2.4545.12) from the Communauté Française de Belgique. Computer time was made available by PRACE-3IP project ThermoSpin on ARCHER (3IP FP7 RI-312763), Belgian CECI, and SEGI-ULg.

*Corresponding author.
gabriele.davino@gmail.com

[1] S. Horiuchi and Y. Tokura, Nat. Mater. **7**, 357 (2008).
[2] S. Horiuchi, Y. Okimoto, R. Kumai, and Y. Tokura, Science **299**, 229 (2003).
[3] K. Kobayashi, S. Horiuchi, R. Kumai, F. Kagawa, Y. Murakami, and Y. Tokura, Phys. Rev. Lett. **108**, 237601 (2012).
[4] F. Kagawa, S. Horiuchi, H. Matsui, R. Kumai, Y. Onose, T. Hasegawa, and Y. Tokura, Phys. Rev. Lett. **104**, 227602 (2010).
[5] F. Kagawa, S. Horiuchi, M. Tokunaga, J. Fujioka, and Y. Tokura, Nat. Phys. **6**, 169 (2010).
[6] T. Miyamoto, H. Yada, H. Yamakawa, and H. Okamoto, Nat. Commun. **4**, 2586 (2013).
[7] E. Collet, M.-H. Leme-Cailleau, M. Buron-Le Cointe, H. Cailleau, M. Wulff, T. Luty, S.-Y. Koshihara, M. Meyer, L. Toupet, P. Rabiller, and S. Techert, Science **300**, 612 (2003).
[8] H. Uemura and H. Okamoto, Phys. Rev. Lett. **105**, 258302 (2010).
[9] T. Miyamoto, K. Kimura, T. Hamamoto, H. Uemura, H. Yada, H. Matsuzaki, S. Horiuchi, and H. Okamoto, Phys. Rev. Lett. **111**, 187801 (2013).
[10] J. B. Torrance, J. E. Vazquez, J. J. Mayerle, and V. Y. Lee, Phys. Rev. Lett. **46**, 253 (1981).
[11] J. B. Torrance, A. Girlando, J. J. Mayerle, J. I. Crowley, V. Y. Lee, P. Batail, and S. J. LaPlaca, Phys. Rev. Lett. **47**, 1747 (1981).
[12] A. Girlando, A. Painelli, S. Bewick, and Z. Soos, Synth. Met. **141**, 129 (2004).
[13] A. S. Tayi, A. K. Shveyd, A. C.-H. Sue, J. M. Szarko, B. S. Rolczynski, D. Cao, T. J. Kennedy, A. A. Sarjeant, C. L. Stern, W. F. Paxton, W. Wu, S. K. Dey, A. C. Fahrenbach, J. R. Guest, H. Mohseni, L. X. Chen, K. L. Wang, J. F. Stoddart, and S. I. Stupp, Nature (London) **488**, 485 (2012).
[14] S. Horiuchi, Y. Tokunaga, G. Giovannetti, S. Picozzi, H. Itoh, R. Shimano, R. Kumai, and Y. Tokura, Nature (London) **463**, 789 (2010).
[15] S. Horiuchi, F. Kagawa, K. Hatahara, K. Kobayashi, R. Kumai, Y. Murakami, and Y. Tokura, Nat. Commun. **3**, 1308 (2012).
[16] A. Painelli and A. Girlando, Phys. Rev. B **37**, 5748 (1988).
[17] Z. G. Soos and A. Painelli, Phys. Rev. B **75**, 155119 (2007).
[18] R. Resta, Phys. Rev. Lett. **80**, 1800 (1998).
[19] L. Del Freo, A. Painelli, and Z. G. Soos, Phys. Rev. Lett. **89**, 027402 (2002).
[20] Z. G. Soos, S. A. Bewick, A. Peri, and A. Painelli, J. Chem. Phys. **120**, 6712 (2004).
[21] G. D'Avino, M. Masino, A. Girlando, and A. Painelli, Phys. Rev. B **83**, 161105 (2011).
[22] G. D'Avino, A. Girlando, A. Painelli, M.-H. Lemée-Cailleau, and Z. G. Soos, Phys. Rev. Lett. **99**, 156407 (2007).
[23] The infinite-correlation limit excludes double ionizations:$D^{2+}A^{2-}$. Specifically, we consider $\Delta, U \to \infty$ with finite $\Gamma_{\rm eff} = \Delta - U/2$, where U is the on-site repulsion and 2Δ is the energy difference between the orbitals of D and A molecules.
[24] A. Painelli and A. Girlando, J. Chem. Phys. **87**, 1705 (1987).
[25] P. Garcia, S. Dahaoui, C. Katan, M. Souhassou, and C. Lecomte, Faraday Discuss. **135**, 217 (2007).
[26] M. Le Cointe, M. H. Lemée-Cailleau, H. Cailleau, B. Toudic, L. Toupet, G. Heger, F. Moussa, P. Schweiss, K. H. Kraft, and N. Karl, Phys. Rev. B **51**, 3374 (1995).
[27] M. J. Frisch *et al.*, GAUSSIAN09 Revision D.1, Gaussian Inc., Wallingford , CT, 2009.
[28] A. E. Reed, R. B. Weinstock, and F. Weinhold, J. Chem. Phys. **83**, 735 (1985).
[29] See Supplemental Material at http://link.aps.org/supplemental/10.1103/PhysRevLett.113.237602, for details.
[30] E. V. Tsiper and Z. G. Soos, Phys. Rev. B **64**, 195124 (2001).
[31] G. D'Avino, L. Muccioli, C. Zannoni, D. Beljonne, and Z. G. Soos, J. Chem. Theory Comput. **10**, 4959 (2014)
[32] $\varepsilon_q = 0.40$, 0.56, 0.51 and 0.37 eV for TTF-CA, $A1$-$D2$, $A1$-$D3$, and $A1$-$D4$, respectively, from B3LYP/6–31 + G* calculations [29].
[33] G. Giovannetti, S. Kumar, A. Stroppa, J. van den Brink, and S. Picozzi, Phys. Rev. Lett. **103**, 266401 (2009).
[34] S. Ishibashi and K. Terakura, Physica (Amsterdam) **405B**, S338 (2010).
[35] A. Girlando, F. Marzola, C. Pecile, and J. B. Torrance, J. Chem. Phys. **79**, 1075 (1983).
[36] G. Catalan and J. F. Scott, Nature (London) **448**, E4 (2007).
[37] J. F. Scott, J. Phys. Condens. Matter **20**, 021001 (2008).
[38] F. Ishii, N. Nagaosa, Y. Tokura, and K. Terakura, Phys. Rev. B **73**, 212105 (2006).